Measurement of the interwell carrier transport lifetime in multiquantum-well optical amplifiers by polarization-resolved four-wave mixing

Roberto Paiella,[a] Guido Hunziker, and Kerry J. Vahala
Department of Applied Physics, Mail Stop 128-95, California Institute of Technology, Pasadena, California 91125

Uzi Koren
Bell Laboratories, Lucent Technologies, Holmdel, New Jersey 07733

(Received 27 August 1996; accepted for publication 30 October 1996)

Polarization-resolved four-wave mixing spectroscopy is used to study interwell carrier dynamics in an alternating-strain multiquantum-well optical amplifier. The experimental data are found to be in good agreement with a simple model based on quantum capture/escape and diffusion processes. The results suggest that the interwell transport in this structure is mainly limited by carrier escape, and give an estimate of 16 ps for the overall transport lifetime. © *1996 American Institute of Physics.* [S0003-6951(96)04753-5]

Interwell carrier transport in semiconductor multiquantum-well structures is a highly nonlinear process with significant implications to the use of these structures in electrical and optical devices. Of particular interest is the finite rate at which the carrier densities in neighboring wells reach equilibrium with one another and with the distribution of unconfined carriers in the barrier region. This process has received considerable attention in recent years[1–8] since it has been associated with nonlinear gain compression, and hence the maximum modulation bandwidth of quantum-well lasers.

In this letter, we report on a simple experiment aimed at measuring the rate at which modulated carrier distributions are transferred between neighboring quantum wells. This measurement is based on polarization-resolved four-wave mixing (FWM) spectroscopy in an InGaAsP alternating-strain semiconductor optical amplifier (SOA), consisting of three pairs of tensile and compressively strained quantum wells.[9] In a recent article[7] it was shown how this technique enables selective excitation and probing of adjacent quantum wells, and the effect of interwell transport was qualitatively observed. Here we apply the results of a subsequent detailed study of the polarization properties of FWM[10] to also obtain quantitative information. In particular, a fit of the experimental data to a simple model gives an estimated 16 ps for the interwell transport lifetime in the structure measured.

Four-wave mixing in SOAs[11,12] can be described as a two-step process as follows: first, beating of the input pump and probe waves (of frequencies ω_p and ω_q, respectively) gives rise to gain and index modulation at the detuning frequency $\Omega=\omega_p-\omega_q$; the pump is then partially scattered by this modulation into a new field harmonic at frequency $\omega_s=\omega_p+\Omega$. In the experiment described here we consider only detuning frequencies below 100 GHz, for which the gain and index modulation mainly results from modulation of the carrier density as a whole[12] (whereas at larger detuning frequencies other FWM processes, such as carrier heating and spectral hole burning, become predominant). In this case, as shown in Ref. 10, modulation only occurs either through beating of the TE components of the input waves or, separately, through beating of their TM components. Furthermore, the TE (TM) component of the pump is then scattered only into a TE (TM) polarized FWM signal. In other words, the FWM susceptibility tensor, defined so that the induced polarization density at ω_s is given by $P_i^s=\chi_{ijkl}E_j^pE_k^p(E_l^q)^*$ (where the indexes j and k refer to the pump components involved in the scattering process and the modulation process, respectively) is subject to the selection rule $\chi_{ijkl}=\delta_{i,j}\delta_{k,l}\chi_{iikk}$.

Based on these considerations, a simple FWM configuration which is particularly well suited to studying interwell transport consists of a TM polarized probe E^q and a linearly polarized pump with equal TE and TM components E^p. In this case, modulation of the carrier densities can only occur through beating of the TM components, and since compressive wells have negligible gain for TM polarized light, this can only take place in the tensile wells; here each polarization component of the pump is subsequently scattered into the same component of the FWM signal. In addition, the modulated carrier distributions from each tensile well are coupled into the neighboring compressive wells, where only a TE polarized FWM signal can be generated. As a result, the TE (E_1^s) and TM (E_2^s) components of the overall FWM signal have the general form

$$E_1^s=R_{1122}(\chi_{1122}^T+\chi_{1122}^{C\leftarrow T})(E^p)^2(E^q)^*,$$
$$E_2^s=R_{2222}\chi_{2222}^T(E^p)^2(E^q)^*, \tag{1}$$

where the superscripts T and C refer to the tensile and the compressive wells, respectively, and $\chi_{11ii}^{C\leftarrow T}$ describes the FWM process in which the modulation is generated in a tensile well and transferred to a compressive well where the pump is then scattered. The prefactors R_{iikk} in these equations account for wave propagation effects and can be regarded as independent of the detuning frequency over the small detuning range (<100 GHz) considered in this work.[10] A schematic representation of the polarization components of the input waves involved in the modulation and scattering processes in each type of well is given in Fig. 1.

The crucial point here is that the contribution to the FWM signal involving interwell transport (whose strength is

[a]Electronic mail: robertop@cco.caltech.edu

 0003-6951/96/69(27)/4142/3/$10.00 © 1996 American Institute of Physics
Downloaded¬20¬Dec¬2005¬to¬131.215.225.171.¬Redistribution¬subject¬to¬AIP¬license¬or¬copyright,¬see¬http://apl.aip.org/apl/copyright.jsp

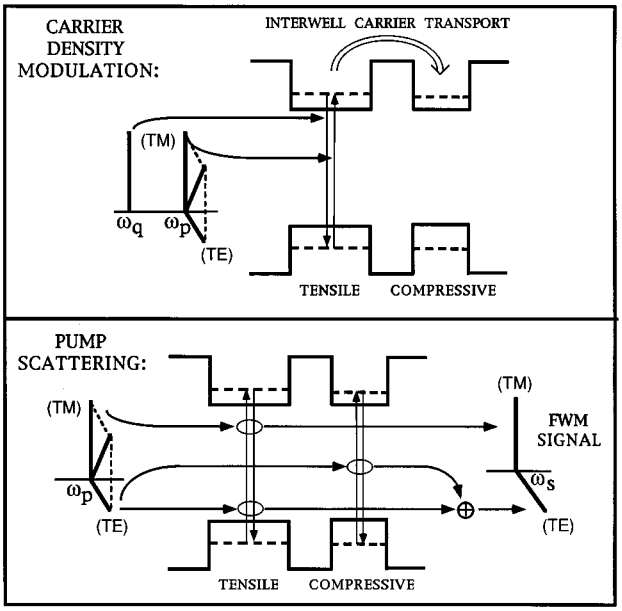

FIG. 1. Schematics of the FWM processes taking place with the input polarizations used in this work. As shown in the upper panel, modulation of the carrier density is generated directly (through beating of the TM components of the input waves) only in the tensile wells, from which it can then be transferred to a neighboring compressive well. Each polarization component of the pump is then correspondingly scattered into the same component of the FWM signal as shown in the lower panel.

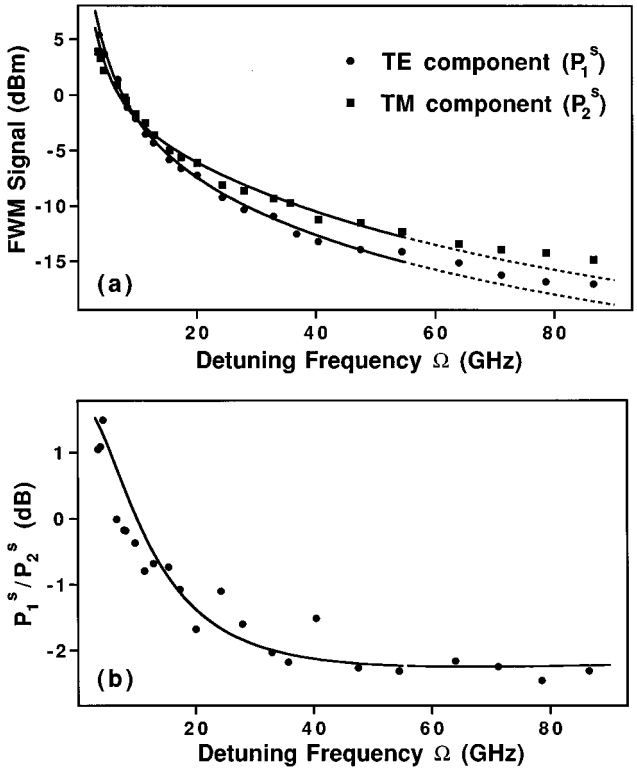

FIG. 2. (a) Optical powers in the TE (circles) and TM (squares) components of the FWM signal, and (b) their ratio vs detuning frequency. The continuous lines are fits to the model theory discussed. As emphasized by the dashing, the fit becomes inaccurate in (a) at detuning frequencies above 50 GHz, where carrier heating, not included in the model, becomes important. However, since its contribution is approximately the same for both the TE and TM components, the fit remains good for their ratio in (b). An approximate transport lifetime of 16 ps is inferred from the data.

proportional to $|\chi_{1122}^{C\leftarrow T}|$) becomes negligible relative to the other contributions at detuning frequencies larger than the interwell transport rate. In this detuning range the probability of a modulated carrier distribution being coupled between neighboring wells within a few modulation periods is negligibly small. As a result, a plot of $P_1^s/P_2^s \propto |(\chi_{1122}^T+\chi_{1122}^{C\leftarrow T})/\chi_{2222}^T|^2$ (P_i^s denoting the optical power in the ith component of the FWM signal) vs Ω should display a low-detuning feature that decays towards a constant value (proportional to $|\chi_{1122}^T/\chi_{2222}^T|^2$) with increasing detuning frequency. This prediction was verified using a high sensitivity optical heterodyne detection system similar to that described in Ref. 12. Figure 2(a) shows the measured optical powers in the TE and TM components of the FWM signal as a function of detuning frequency; their ratio P_1^s/P_2^s is plotted in Fig. 2(b). The contribution associated with coupling of the carrier density modulation from the tensile to the compressive wells is clearly seen at low detuning frequencies, and becomes negligible at $\Omega \approx 40$ GHz.

In order to extract quantitative information from these data, we consider a simple model for the interwell carrier dynamics. The transfer of carriers between adjacent wells mainly results from phonon-assisted quantum capture/escape processes between the quantum well states and the overlying continuum of 3D states of the SOA waveguide layer.[3,4] We assume that the 2D states of each well are coupled to wave packets of 3D states localized near the same well, whose dynamics is dominated by classical diffusion (drift is of minor importance in a forward-biased structure);[3,4] any other interwell transport mechanism such as tunneling is also neglected. Finally, the dynamics of holes (which are known to have a shorter capture lifetime[4]) is assumed to adiabatically follow that of the electrons and is not considered explicitly.

These assumptions lead to the following set of rate equations

$$
\begin{aligned}
-i\Omega N_{2\mathrm{D}}^T &= -\left(\frac{1}{\tau_s}+\frac{1}{\tau_{esc}^T}\right)N_{2\mathrm{D}}^T+\frac{N_{3\mathrm{D}}^T}{\tau_{cap}^T} \\
&\quad -\frac{\epsilon_0 cn}{2}\frac{g_2^T}{\hbar\omega_p}E^p(E^q)^*, \qquad (2)\\
-i\Omega N_{2\mathrm{D}}^C &= -\left(\frac{1}{\tau_s}+\frac{1}{\tau_{esc}^C}\right)N_{2\mathrm{D}}^C+\frac{N_{3\mathrm{D}}^C}{\tau_{cap}^C}.
\end{aligned}
$$

Here $N_{2\mathrm{D}}$ ($N_{3\mathrm{D}}$) is the harmonic component at the detuning frequency Ω of the density of electrons confined inside (unconfined but localized near) the quantum well under consideration; τ_s, τ_{esc}, and τ_{cap} are the recombination, escape, and capture lifetimes, respectively; and again the superscripts T and C distinguish between quantities of tensile and compressive wells (in what follows we assume that the time constants do not depend on the type of well). The last term on the right-hand side of the top equation (where g_2 is the gain coefficient for TM polarized waves and n is the background refractive index) accounts for modulation of the carrier density by beating of the input waves in each tensile well; no such term is present in the bottom equation for the

Downloaded¬20¬Dec¬2005¬to¬131.215.225.171.¬Redistribution¬subject¬to¬AIP¬license¬or¬copyright,¬see¬http://apl.aip.org/apl/copyright.jsp

FWM polarization configuration used in this work. Finally, the density of unconfined electrons N_b in the SOA waveguide satisfies the diffusion equation

$$-i\Omega N_b = -\frac{N_b}{\tau_s} + D\frac{d^2 N_b}{dz^2}, \tag{3}$$

subject to the boundary conditions $N_b(z_i^T \pm L_w^T/2) = N_{3D}^T$ and $DdN_b/dz\,(z_i^T \pm L_w^T/2) = \pm L_w^T/2\,(N_{3D}^T/\tau_{cap}^T - N_{2D}^T/\tau_{esc}^T)$ near the center z_i^T of the ith tensile well, of width L_w^T (and similarly for each compressive well).[13]

The connection between the simple model of interwell dynamics just presented and the FWM experimental results of Fig. 2 is provided by Eq. (1) plus the relations $\chi_{jj22}^T \propto N_{2D}^T$ and $\chi_{1122}^{C\leftarrow T} \propto N_{2D}^C$, where the proportionality constants are essentially independent of Ω, and can be evaluated following Ref. 11. The continuous lines in Fig. 2 are the complete theoretical fits. Aside from unimportant multiplicative prefactors, the only physical parameters important in determining these curves are the capture and escape lifetimes, which are taken here to be $\tau_{cap}=1.5$ ps, and $\tau_{esc}=8$ ps, respectively. On the other hand, the fits are relatively insensitive to the recombination lifetime τ_s and to the diffusion constant D, as long as the diffusion length $L_D = |\sqrt{D\tau_s/(1-i\Omega\tau_s)}|$ is much larger than the barrier width L_b (100 Å in the SOA under study), which is certainly the case for $\Omega < 100$ GHz. The agreement with the experimental data is excellent, except for the points at detuning frequencies in excess of about 50 GHz, where carrier heating (not included in our model) is known[12] to cause an increase in the FWM conversion efficiency. Note, however, that since this increase is approximately the same for both the TE and TM components, the fit remains good for their ratio in Fig. 2(b).

The application of the above model directly provides a numerical estimate of the interwell transport rate. A detailed expression for this quantity can be obtained by using the solution to the boundary-value problem of Eq. (3) to eliminate the 3D carrier densities from Eq. (2). This procedure introduces in the rate equation for N_{2D}^C a term proportional to N_{2D}^T (and vice versa), whose proportionality constant $1/\tau_t^{C\leftarrow T}$ (more precisely its magnitude) is then an effective rate for the overall transport of modulated carrier distributions from a tensile well to a neighboring compressive well. Taking the limit $L_D \gg L_b$ and averaging over the properties of the two types of wells, we find the simplified expression

$$\frac{1}{\tau_t} = \frac{1}{2\tau_{esc}}\,\frac{1}{1-i\Omega\tau_{cap}L_b/L_w}, \tag{4}$$

which makes intuitive sense. In particular, at low detuning frequencies, where diffusion may be regarded as instantaneous, interwell transport is mainly limited by escape (capture is always faster[4]), and $\tau_t = 2\tau_{esc} \approx 16$ ps (the factor of two appears because, if both types of wells have the same capture lifetime, each escaped carrier from a well can be transferred to an adjacent well or recaptured in the same well with equal probability).[14]

In conclusion, the FWM experiment described here combined with a simple model allowed us to study the interwell transport lifetime for modulated carrier distributions in an alternating-strain SOA. We found that this lifetime is mainly determined by quantum escape from each well. Furthermore, we estimated $\tau_t \approx 16$ ps for modulation frequencies smaller than $L_w/(L_b 2\pi\tau_{cap}) \approx 80$ GHz (beyond this value, τ_t decreases with increasing modulation frequency).

The authors acknowledge R. M. Jopson for coating the device used in these experiments, also D. Geraghty and R. B. Lee for stimulating discussions. This work was supported by ARPA (Contract No. DAAL 01-94-K-03430) and the National Science Foundation (Grant No. ECS-9412862).

[1] W. Rideout, W. F. Sharfin, E. S. Koteles, M. O. Vassell, and B. Elman, IEEE Photonics Technol. Lett. **3**, 784 (1991).
[2] R. Nagarajan, T. Fukushima, S. W. Corzine, and J. E. Bowers, Appl. Phys. Lett. **59**, 1835 (1991).
[3] S. Weiss, J. M. Wiesenfeld, D. S. Chemla, G. Raybon, G. Sucha, M. Wegener, G. Eisenstein, C. A. Burrus, A. G. Dentai, U. Koren, B. I. Miller, H. Temkin, R. A. Logan, and T. Tanbun-Ek, Appl. Phys. Lett. **60**, 9 (1992).
[4] S. C. Kan, D. Vassilovski, T. C. Wu, and K. Y. Lau, Appl. Phys. Lett. **61**, 752 (1992).
[5] D. Vassilovski, T. C. Wu, S. C. Kan, K. Y. Lau, and C. E. Zah, Appl. Phys. Lett. **63**, 2307 (1993).
[6] N. Tessler and G. Eisenstein, IEEE J. Quantum Electron. **29**, 2230 (1993).
[7] J. Zhou, N. Park, K. J. Vahala, M. A. Newkirk, and B. I. Miller, Appl. Phys. Lett. **65**, 1897 (1993).
[8] G. Lenz, E. P. Ippen, J. M. Wiesenfeld, M. A. Newkirk, and U. Koren, Appl. Phys. Lett. **68**, 2933 (1996).
[9] M. A. Newkirk, B. I. Miller, U. Koren, M. G. Young, M. Chen, R. M. Jopson, and C. A. Burros, IEEE Photonics Technol. Lett. **4**, 406 (1993).
[10] R. Paiella, G. Hunziker, J. Zhou, K. J. Vahala, U. Koren, and B. I. Miller, IEEE Photonics Technol. Lett. **8**, 773 (1996).
[11] G. P. Agrawal, J. Opt. Soc. Am. B **5**, 147 (1988).
[12] J. Zhou, N. Park, J. W. Dawson, K. J. Vahala, M. A. Newkirk, and B. I. Miller, Appl. Phys. Lett. **63**, 1179 (1993).
[13] Implicit in these boundary conditions are the two main simplifications of the model, namely (I) a periodic chain of pairs of oppositely strained wells is assumed, and (II) the finite width of the well is not considered in treating the diffusion process.
[14] It is important to point out that the expressions used to fit the data depend on τ_{esc} and τ_{cap} only through the interwell transport rate of Eq. (4) (and a similarly defined effective escape rate). The theoretical fits then directly give us an estimate of τ_t (as a single-pole function of Ω), regardless of the detailed form of Eq. (4). The numerical values quoted above for τ_{esc} and τ_{cap} on the other hand do depend on the details of Eq. (1) and as such further rely on the simplifying assumptions of the model.

Downloaded¬20¬Dec¬2005¬to¬131.215.225.171.¬Redistribution¬subject¬to¬AIP¬license¬or¬copyright,¬see¬http://apl.aip.org/apl/copyright.jsp